COMPARISON OF NONCOHERENT DETECTORS FOR SOQPSK AND GMSK IN PHASE NOISE CHANNELS

Afzal Syed
Department of Electrical Engineering & Computer Science
University of Kansas
Lawrence, KS 66046
afzal@ittc.ku.edu

Faculty Advisor:
Erik Perrins

ABSTRACT

SOQPSK and GMSK are highly bandwidth efficient continuous phase modulation (CPM) schemes with several desirable qualities. In both cases, coherent detectors are available with good performance in AWGN. In this paper, we develop reduced complexity noncoherent detectors for SOQPSK and GMSK; and discuss a phase noise model. This is followed by a performance comparison of both the noncoherent detectors in channels with phase noise.

INTRODUCTION

Shaped-offset QPSK is a highly bandwidth efficient modulation in which data transmissions on the *in-phase* (I) and *quadrature* channels are offset by half a symbol time. Thus there are no instantaneous 180° phase shifts and a higher degree of spectral containment results [1]. In SOQPSK the phase transitions are continuous rather than instantaneous as in the case of OQPSK, making it more bandwidth efficient. SOQPSK has been incorporated into military and aeronautical telemetry standards and it is applicable in any setting where bandwidth-efficient constant-envelope modulations are needed. The use of longer, smoother frequency pulses can make SOQPSK more bandwidth efficient at the expense of receiver complexity.

Guassian Minimum shift-keying (GMSK) is another important form of continuous phase modulation [2, 3] which is widely used in wireless communication systems because of its spectral efficiency and constant envelope property [4]. GMSK has been adopted as the digital modulation scheme for the European global system for mobile communications(GSM) [5, 6]. GMSK can achieve a tradeoff among bandwith efficiency, power efficiency, and detector complexity by appropriately configuring the bandwidth-time BT product [4, 7]. GSM uses $BT = 0.3$, a lower BT results in a more bandwith-efficient GMSK signal.

Noncoherent receivers are preferred because they are easy to synchronize and are more robust. Both SOQPSK and GMSK have good performance in AWGN, however there has not been much published about how noncoherent receivers for these modulation schemes perform in phase noise. In this paper we investigate the performance of noncoherent detectors for these modulation schemes in the presence of phase noise. We start by developing coherent detectors for military standard SOQPSK (SOQPSK-MIL), which is full-response. For the partial response version used in aeronautical telemetry (SOQPSK-TG), the optimal detector requires a trellis of 512 states [8], we use a reduced-complexity option for SOQPSK-TG known as the frequency pulse truncation technique [9]. This allows us to use the same simple 4-state trellis that we use for the MIL case with a minor loss of 0.2 dB. We then develop a reduced complexity coherent

detector for GMSK which achieves optimal performance and go on to construct noncoherent detectors.

In the next section we give the signal models for SOQPSK and GMSK. Then we discuss the trellis and coherent detectors for SOQPSK and GMSK. We develop noncoherent detectors for SOQPSK and GMSK and examine their performance under a simple channel model with varying carrier phase.

SIGNAL MODEL

A. CPM

We will use complex-baseband notation to represent various signals, all CPM signals can be described as [3]

$$s(t;\boldsymbol{\alpha}) \triangleq \exp\{j\psi(t;\boldsymbol{\alpha})\} \tag{1}$$

where the phase is a pulse train of the form

$$\psi(t;\boldsymbol{\alpha}) \triangleq 2\pi h \sum_i \alpha_i q(t-iT) \tag{2}$$

and α_i is an M-ary transmitted symbol, T is the duration of each α_i , and h is the modulation index. The *phase pulse* $q(t)$ is thought of as the time-integral of a *frequency pulse* $f(t)$ with area 1/2 and duration LT and is given by

$$q(t) \triangleq \begin{cases} 0 & t<0 \\ \displaystyle\int_0^t f(\tau)\,d\tau & 0 \le t < LT \\ 1/2 & t \ge LT_s \end{cases} \tag{3}$$

when $L=1$ the signal is *full-response* and when $L>1$ it is *partial response*. Due to the constraints on $f(t)$ and $q(t)$, and assuming a rational modulation index $h=2k/p$, the phase may be expressed as

$$\psi(t;\boldsymbol{\alpha}) = \underbrace{2\pi h \sum_{i=n-L+1}^{n} \alpha_i q(t-iT_s)}_{\theta(t)} + \underbrace{\pi h \sum_{i=0}^{n-L} \alpha_i}_{\theta_{n-L}} \tag{4}$$

where $nT \le t < (n+1)T$. The *phase state* θ_{n-L} can assume only p distinct values given by the look up table

$$\theta[x] = \frac{2\pi x}{p}, \qquad 0 \le x < p-1. \tag{5}$$

B. SOQPSK

For SOQPSK, α_i is drawn from a ternary alphabet, i.e $\alpha_i \in \{-1,0,+1\}$, where $M=3$. The modulation index is $h=1/2$. In this paper we discuss two versions of SOQPSK, SOQPSK-MIL [10], which is full response ($L=1$) with a rectangular shaped frequency pulse

$$f_{\text{MIL}}(t) = \begin{cases} \frac{1}{2T}, & 0 \le t < T \\ 0, & \text{otherwise.} \end{cases} \tag{6}$$

The second, SOQPSK-TG [11, 12], is partial-response with $L=8$ and has a frequency pulse given by

$$f_{\text{TG}}(t) \triangleq A\frac{\cos(\frac{\pi\rho Bt}{2T})}{1-4(\frac{\rho Bt}{2T})^2} \times \frac{\sin(\frac{\pi Bt}{2T})}{\frac{\pi Bt}{2T}} \times w(t) \tag{7}$$

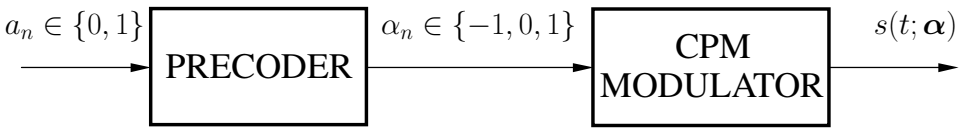

Figure 1: Signal model for SOQPSK.

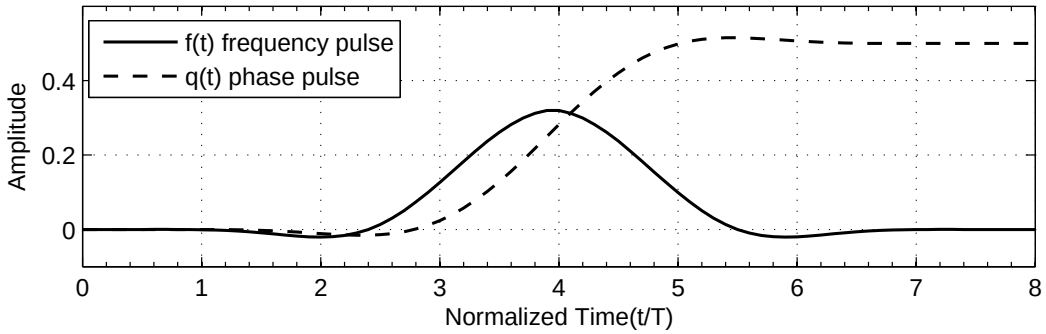

Figure 2: The length-8T frequency and phase pulses for SOQPSK-TG.

where the window is

$$w(t) \triangleq \begin{cases} 1, & 0 \le |\frac{t}{2T}| < T_1 \\ \frac{1}{2} + \frac{1}{2}\cos(\frac{\pi}{T_2}(\frac{t}{2T} - T_1)), & T_1 \le |\frac{t}{2T}| \le T_1 + T_2 \\ 0, & T_1 + T_2 < |\frac{t}{2T}| \end{cases} \tag{8}$$

The constant A is chosen such that the area of the pulse is equal to $1/2$ and $T_1 = 1.5$, $T_2 = 0.5$, $\rho = 0.7$ and $B = 1.25$. Figure 2 shows the frequency pulse $f_{\text{TG}}(t)$ and corresponding phase pulse $q_{\text{TG}}(t)$.

SOQPSK is different from ordinary CPM in that ternary data are the output of a precoder as shown in Figure 1. The precoder converts binary data $a_n \in \{0,1\}$ into ternary data α_i according to the mapping [13]

$$\alpha_n = (-1)^{n+1}(2a_{n-1} - 1)(a_n - a_{n-2}). \tag{9}$$

The precoder orients the phase of the CPM signal in (1) such that the inphase and quadrature bits can be recovered using a standard OQPSK detector. Also a_n are differentially encoded bits according to [14].

C. GMSK

GMSK is an important form of CPM [3], the signal model is same as (1) through (5). The frequency pulse $f(t)$ for GMSK is given by

$$f(t) = \frac{1}{2T}\left\{Q\left[2\pi B_b \frac{t - T/2}{(\ln 2)^{1/2}}\right] - Q\left[2\pi B_b \frac{t + T/2}{(\ln 2)^{1/2}}\right]\right\} \tag{10}$$

where the parameter B_b is arbitrary and set to obtain desired distance or spectral properties and

$$Q(t) = \int_t^\infty \frac{1}{(2\pi)^{1/2}} e^{-\tau^2/2}\, d\tau. \tag{11}$$

In this paper we use GMSK with $BT = 0.25$, $L = 4$ and $h = 1/2$. Figure 3 shows the frequency pulse GMSK $f(t)$ and corresponding phase pulse $q(t)$. The reason for choosing GMSK with this BT product is that its performance in an AWGN channel is very similar to that of SOQPSK.

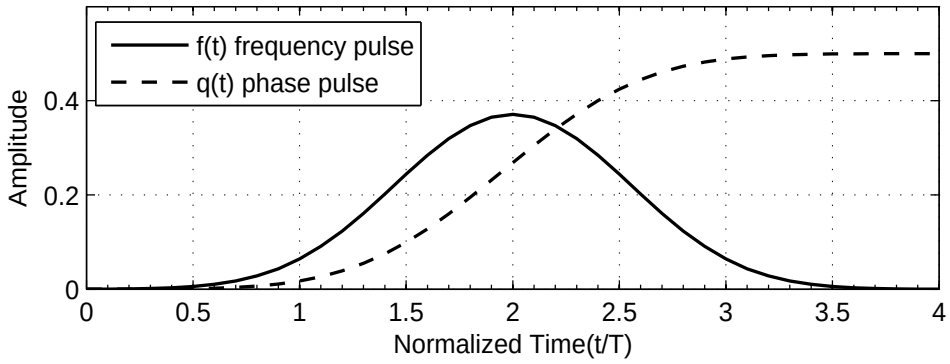

Figure 3: The length-4T frequency and phase pulses for GMSK.

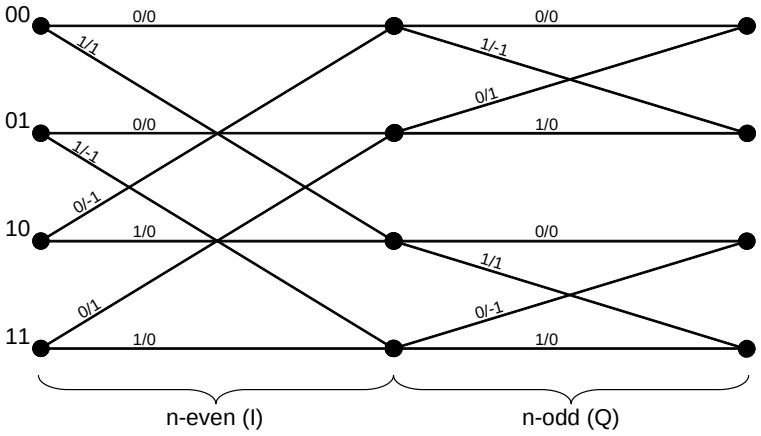

Figure 4: 4-state time-varying trellis for the precoder/CPM Modulator The labels along the branches are for the input bit/output symbol pair a_n/α_n.

COHERENT DETECTOR MODELS

Although our final objective is to arrrive at noncoherent detectors for SOQPSK and GMSK, we will first examine coherent detectors. This will yield useful models based on which the noncoherent detectors will be built.

A. Coherent Detection Algorithm for Full-Response SOQPSK

The precoder in (9) can be described with an 8-state trellis, where three binary-valued state variables are needed: n-even/n-odd, a_{n-1} and a_{n-2}. If we construct a *time-varying* trellis, with different sections for n-even and n-odd, then we have the 4 state trellis shown in Figure 4. The labels along each branch show the input bit/output symbol pair, a_n/α_n, for the given branch. The state variables are a_{n-1}, and a_{n-2} and are ordered such that the inphase bit of this pair is always the MSB and the quadrature bit of this pair is always the LSB. When n is even, the branch bit a_n replaces the inphase bit in the state variable, and likewise for the quadrature bit when n is odd.

There is a one-to-one mapping between the trellis state values, in the set $\{00, 01, 10, 11\}$, and the CPM phase state indexes, in the set $\{0, 1, 2, 3\}$ which is shown in Figure 5. It is evident that the CPM phase states are a $\pi/4$-rotated version of the traditional QPSK constellation. This mapping implies that we could

State	P_l
00	3
01	2
10	0
11	1

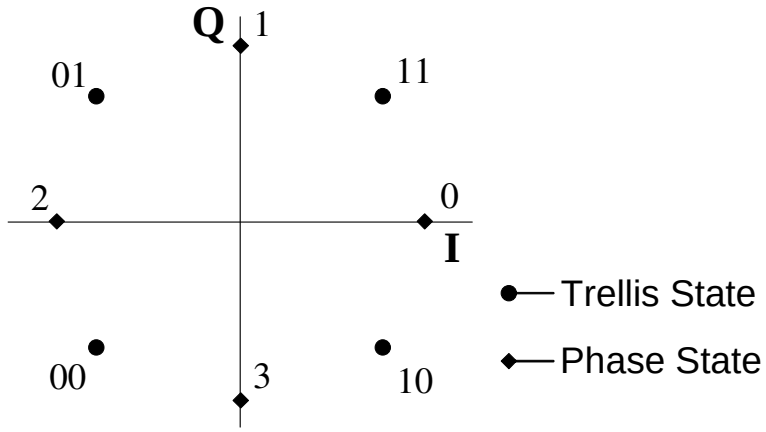

Figure 5: The mapping between the trellis states and the phase state index.

construct a 4-state trellis corresponding to these four CPM phase states. We use the trellis in Figure 4 and the mapping in Figure 5 to obtain the CPM phase state index when required.

With the trellis defined for the system in Figure 1, we outline the optimal detector for the received signal

$$r(t) = s(t;\alpha)e^{j\phi(t)} + n(t) \tag{12}$$

where $n(t)$ is complex-valued additive white Gaussian noise with zero mean and single-sided power spectral density N_0.The phase shift $\phi(t)$ introduced by the channel is unknown in general but for the moment we assume that $\phi(t)$ is zero so as to construct a coherent detector. This condition will be relaxed when we consider the noncoherent detector.

SOQPSK-MIL being full-response, no additional states are required and an optimal maximum likelihood sequence detection (MLSD) detector can be obtained from this 4-state trellis [15]. At the receiving end, each branch of the trellis has a *branch vector* $\tilde{B}_n \triangleq [\tilde{u}_n, \tilde{S}_n]$, which defines the *underlying hypothesis* for the branch. Given this vector, there is a one-to-one correpondence to a hypothesized ending state $\tilde{E}_n \in \{00, 01, 10, 11\}$, a hypothesized branch symbol $\tilde{\alpha}_n$, and a hypothesized phase state θ_{n-1} as shown in Figure 4. The optimal coherent detector for full-response SOQPSK is implemented via the Viterbi algorithm with the recursive metric update [3]

$$\lambda_{n+1}(\tilde{E}_n) \triangleq \lambda_n(\tilde{S}_n) + \text{Re}\{z_n(\tilde{\alpha}_n)e^{-j\tilde{\theta}_n - 1}\} \tag{13}$$

where $\lambda_n(\cdot)$ is the cumulative metric for a given state at index n and $z_n(\tilde{\alpha}_n)$ is a sampled matched filter output

$$z_n(\tilde{\alpha}_n) \triangleq \int_{nT}^{(n+1)T} r(t)e^{-j2\pi h\tilde{\alpha}_n q(t-nT)}\, dt. \tag{14}$$

Three complex-valued matched filters are required for full-response SOQPSK.

B. Detection of Partial-Response SOQPSK-TG

After defining the optimal *coherent* detector for *full*-response SOQPSK, we show the modifications needed to arrive at the *coherent* detector for *partial*-response SOQPSK.

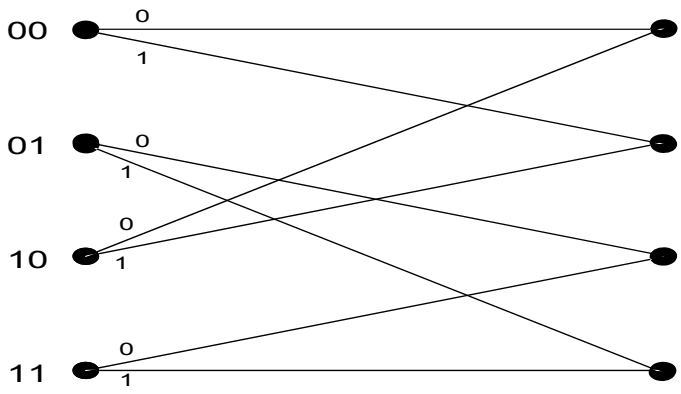

Figure 6: GMSK trellis reduced to 4 states, $\alpha_{n-2}, \alpha_{n-1}$ represent the trellis states. The labels along the branch represent the output symbol α_n

An optimal detector for the TG version of SOQPSK optimal detector requires $p \cdot 2^{L-1}$ or 512 phase states due to the partial-response of the waveform. Instead of using the optimal detector with a 512-state trellis we pursue a near-optimum approximation for SOPQPSK-TG for this paper. The appromixation method we use is frequency pulse truncation (PT) [9] which is based on the 4-state trellis in Figure 4. This approach stems from the fact that frequency pulses which are long and smooth are oftentimes near zero for a significant portion of their duration. This is clearly the case for f_{TG}(t) in Figure 2. We base the detector on a frequency pulse which has been truncated to a duration of one symbol time(full-response). Since the detector uses a *phase* pulse, we translate these arguments accordingly and otain a modified phase pulse

$$q_{\text{PT}}(t) = \begin{cases} 0, & t < 0 \\ q(t + (L-1)T/2), & 0 \le t \le T \\ 1/2, & t > T. \end{cases} \tag{15}$$

Even though the phase pulse in (15) has infinite duration, its time-varying portion has been shortened to the interval $[0, T]$, which gives it full-response behavior. Now, it can be used with the 4-state trellis in Figure 4 and in the full-responce CPM metric (14), which serves as the branch metric increment for the Viterbi algorithm in (13).

C. Reduced Complexity Detector for GMSK

In this section we start with the 32 state trellis for GMSK with $L = 4$ and discuss how it can be reduced to a 4 state trellis.

For GMSK with $BT = 0.25$, we have $L = 4$, $h = 1/2$ and $p = 4$; the number of trellis states would be $S = pM^{L-1}$ or 32. Each state is defined by a 4-tuple $(\theta_{n-4}, \alpha_{n-3}, \alpha_{n-2}, \alpha_{n-1})$, the phase states are given by [3]

$$\theta_{n-L} = h\pi \sum_{i=-\infty}^{n-L} \alpha_i \bmod 2\pi. \tag{16}$$

The first complexity reduction step we peform is truncating the frequency pulse to a duration of 3 symbol times as outlined in the previous section. This would reduce the number of trellis states to 16 defined by the 3-tuple $(\theta_{n-3}, \alpha_{n-2}, \alpha_{n-1})$, each branch is defined by $B_n = (\theta_{n-3}, \alpha_n, \alpha_{n-2}, \alpha_{n-1})$. This trellis can be reduced to a 4 state trellis with the same 8 (as $L = 3$) matched filters by using decision

feedback to find the phase θ_{n-2}. There are two branches which end in each trellis state and the branch which has the higher branch metric is the survivor, with symbol $\hat{\alpha}_{n-2}$, the phase state for the hypothesised ending state can then be estimated using

$$\hat{\theta}_{n-2}(\tilde{E}_n) = \hat{\theta}_{n-3}(\tilde{S}_n) + \pi h \tilde{\alpha}_{n-2}. \tag{17}$$

For such a trellis each state would be defined as $S_n = (\alpha_{n-1}, \alpha_{n-2})$ and branches as $B_n = (\alpha_n, \alpha_{n-1}, \alpha_{n-2})$ as shown in Figure 6. Each trellis state starts off with phase $\theta = 0$ and for each subsequent stage of the trellis the phase is updated using (17).

NONCOHERENT DETECTION ALGORITHM

The assumption that the channel/carrier phase $\phi(t)$ is zero is now relaxed and we assume that it has an unknown but constant value of ϕ_0. The metric in (13) is modified as [16, 17]

$$\lambda_{n+1}(\tilde{E}_n) = \lambda_n(\tilde{S}_n) + \text{Re}\{Q_n^*(\tilde{S}_n) z_n(\tilde{\alpha}_n) e^{-j\tilde{\theta}_n - 1}\} \tag{18}$$

where the complexed-valued *phase reference* $Q_n(\cdot)$ is given by the recursive update

$$Q_{n+1}(\tilde{E}_n) \triangleq a Q_n(\tilde{S}_n) + (1-a) z_n(\tilde{\alpha}_n) e^{-j\tilde{\theta}_{n-1}} \tag{19}$$

with the *forgetting factor a* being a real number in the range $0 < a < 1$.

The phase references are updated after the local surviors at each trellis stage are declared. This algorithm can be used for noncoherent detection of any CPM including SOQPSK(MIL and TG) and GMSK.

PERFORMANCE

This section gives numerical performance results for SOQPSK-MIL, SOQPSK-TG and GMSK. Although we are interested in a noncoherent detector, the natural choice for benchmark is optimal coherent maximum likelihood sequence detection (MLSD). The MLSD probability of bit error for differentially encoded SOQPSK-MIL and SOQPSK-TG using the 4-state time variant trellis and for GMSK is tightly upper-bounded by

$$P_b \leq Q\left(\sqrt{d_0^2 \frac{E_b}{N_0}}\right) + Q\left(\sqrt{d_1^2 \frac{E_b}{N_0}}\right) \tag{20}$$

where E_b/N_0 is the bit-energy-to-noise ratio and $Q(t)$ is given by (11).

For SOQPSK-MIL we have $d_0^2 = 1.73$ [15] and $d_1^2 = 2.36$. For SOQPSK-TG we have $d_0^2 = 1.60$ and $d_1^2 = 2.59$ and for GMSK with $BT = 0.25$ using the 32 state trellis $d_0^2 = 1.689$ and $d_1^2 = 2.3748$.

Since the motivation for a noncoherent receiver is the case when the carrier phase is not known and assumed to be varying [18], a simple model will be introduced for variations in the carrier phase. Let [19]

$$\phi_n \equiv \phi(nT) = \phi_{n-1} + \nu_n \bmod 2\pi \tag{21}$$

where $\{\nu_n\}$ are independent and identically distributed Guassian random variables with zero mean and variance δ^2. This models the phase noise as a first order Markov process with Guassian transition probability distribution. For perfect carrier phase tracking, $\delta = 0$.

Figures 7, 8 and 9 show the performance of noncoherent detectors for SOQPSK and GMSK in phase noise as function of the forgetting factor a, 3 different values of a were chosen to establish a relation

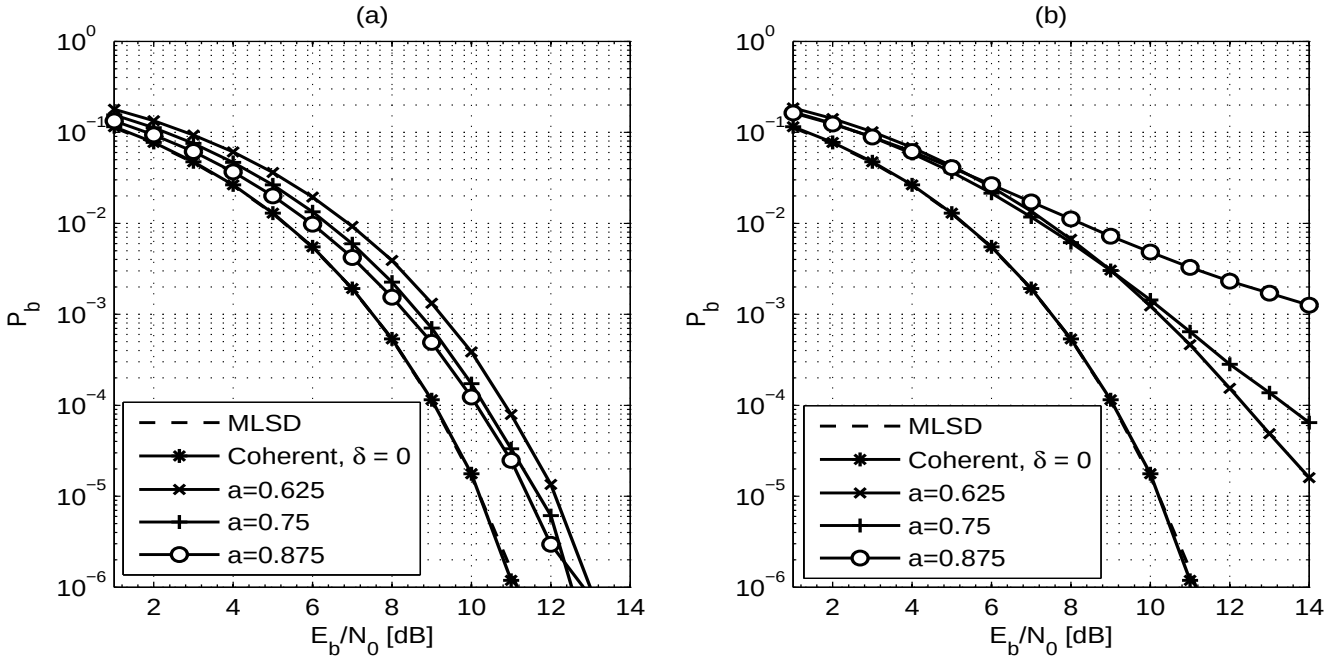

Figure 7: Performance of Noncoherent detector for SOQPSK-MIL with a) $\delta = 2°$/symbol and b) $\delta = 5\ °$/symbol.

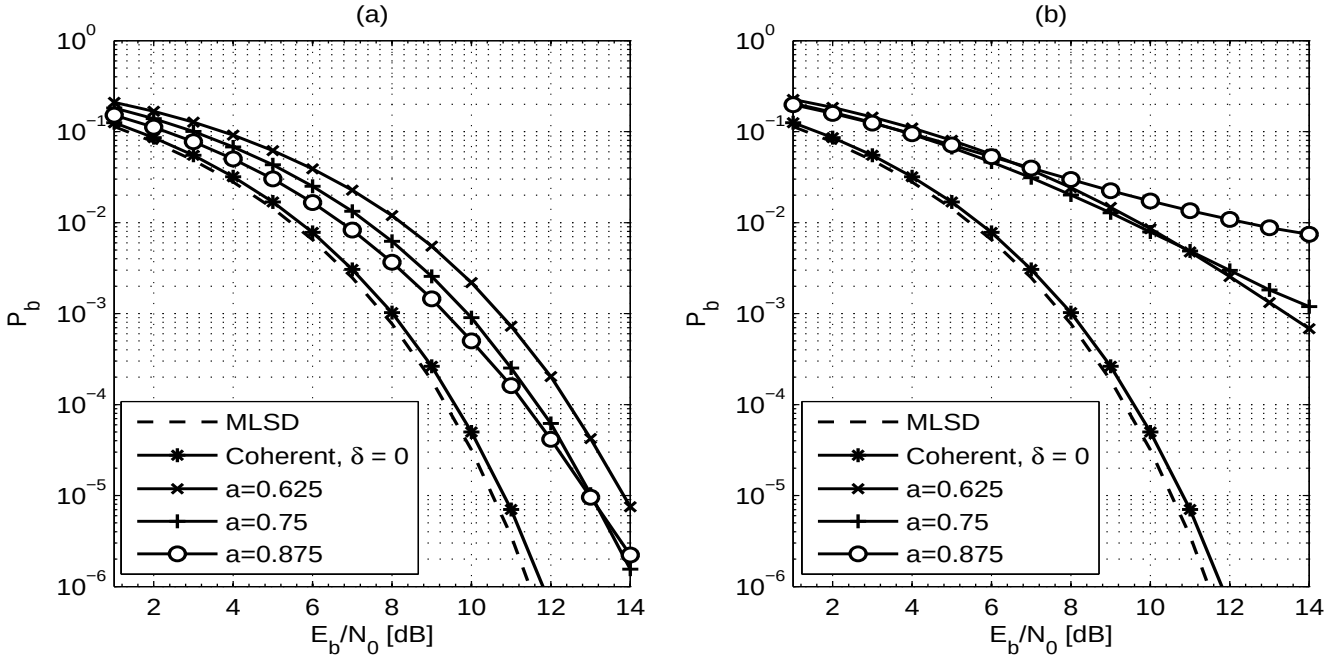

Figure 8: Performance of Noncoherent detector for SOQPSK-TG with a) $\delta = 2°$/symbol and b) $\delta = 5°$/symbol.

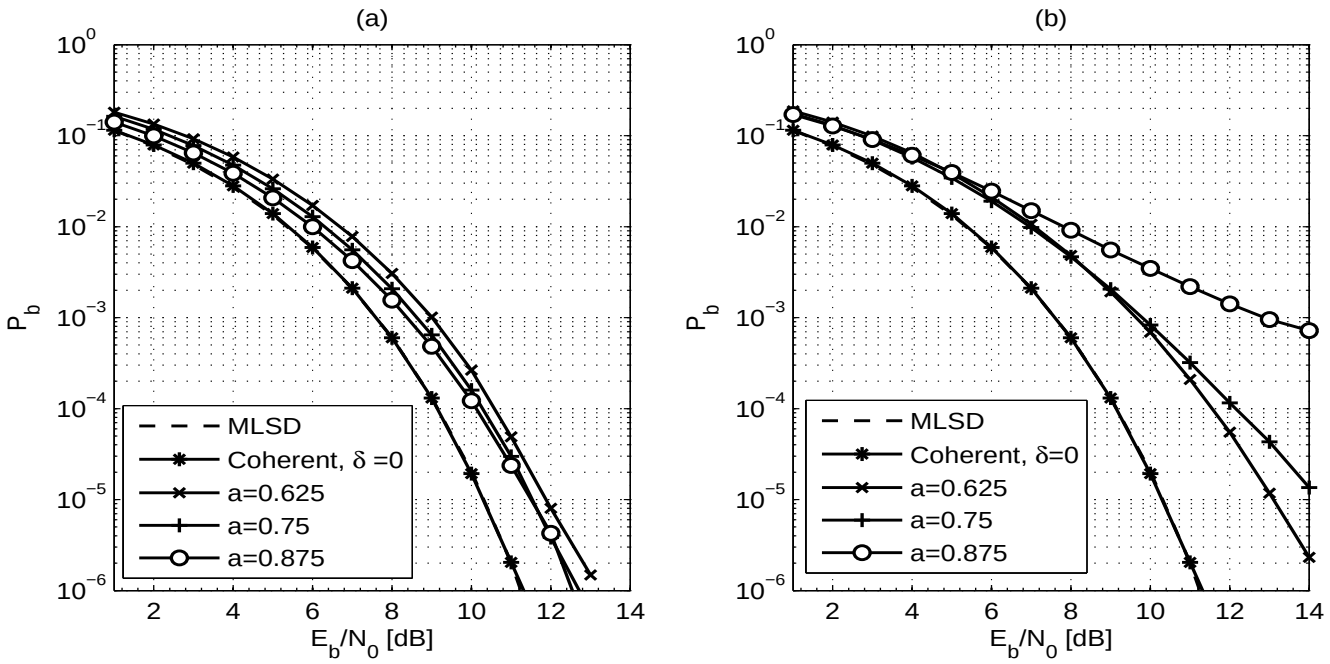

Figure 9: Performance of Noncoherent detector for GMSK with a) $\delta = 2°$/symbol and b) $\delta = 5°$/symbol.

between this design paramater and performance. $\delta = 2°$ / symbol and $\delta = 5°$/symbol were the 2 values chosen for δ.

For the moderate value of $\delta = 2°$/symbol, both the SOQPSK-MIL and GMSK noncoherent detectors show very similar performance, SOQPSK-TG performs significantly poorly. Some of this degradation in performance for noncoherent SOQPSK-TG detector could be attributed to the 0.2 dB [20] loss due to the PT approximation. Also, the loss grows large as a decreases, the best value for a was found to be 0.875. The performance curves for GMSK are relatively close together compared to the SOQPSK curves. The loss measured relative to MLSD at $P_b = 10^{-5}$ for SOQPSK-MIL, GMSK and SOQPSK-TG was found to be 1.6, 1.6 and 2.3 dB respectively.

For the more severe value of $\delta = 5°$/symbol, the loss measured relative to MLSD at $P_b = 10^{-5}$ for SOQPSK-MIL, GMSK and SOQPSK-TG was 4.5, 2.6 and 9.8 dB respectively. Only the GMSK noncoherent detector perfoms satisfactorily, for this case with $a = 0.625$; this implies that as the severity of phase noise increases, a should be chosen to be low, so as to better track phase change.

CONCLUSIONS

We have developed reduced complexity noncoherent detectors for full response and partial response SOQPSK and GMSK. The design includes a time-varying trellis, pulse-truncation, trellis complexity reduction with decision feedback and the noncoherent detection algorithm. We observed that the performance of the noncoherent GMSK detector in presence of phase noise is closer to MLSD GMSK detector than that of noncoherent SOQPSK detectors. When δ of phase noise is $5°$/symbol the noncoherent SOQPSK detectors perform very poorly, this is not the case with noncoherent GMSK detector. Thus in applications where there is phase noise and noncoherent detection is to be used, GMSK is clearly the better choice.

REFERENCES

[1] E. Perrins and M. Rice, "Simple detectors for shaped-offset QPSK using the PAM decomposition," in *Proc. IEEE Global Telecommunications Conf.*, (St. Louis, Missouri), pp. 408–412, Nov./Dec. 2005.

[2] T. Ojanpera and R. Prasad, "An overview of air interface multiple access for IMT-2000/UMTS," *IEEE Commun. Mag.*, vol. 36, pp. 82–95, Sept. 1998.

[3] J. B. Anderson, T. Aulin, and C.-E. Sundberg, *Digital Phase Modulation*. New York: Plenum Press, 1986.

[4] J. Wu and G. Saulnier, "A two-stage MSK-type detector for Low-BT GMSK signals," *IEEE Trans. on Vehicular Technology*, vol. 52, July 2003.

[5] N. Al-Dhahir and G. Saulnier, "A high-performance reduced-complexity GMSK demodulator," *IEEE Trans. Commun.*, vol. 46, pp. 1409–1412, Jan. 1998.

[6] R. Steele, *Mobile Radio Communication*. New York: Pentech, 1995.

[7] R. Fantacci, "Proposal of an interference cancellation receiver with low complexity for DS /CDMA mobile communication systems," *IEEE Trans. on Vehicular Technology*, vol. 48, pp. 1039–1046, July 1999.

[8] M. Geoghegan, "Implementation and performance results for trellis detection of SOQPSK," in *Proc. Int. Telemetering Conf.*, Oct. 2001.

[9] A. Svensson, C.-E. Sundberg, and T. Aulin, "A class of reduced-complexity Viterbi detectors for partial response continuous phase modulation," *IEEE Trans. Commun.*, vol. 32, pp. 1079–1087, Oct. 1984.

[10] D. I. S. Agency, "Department of Defense interface standard, interoperability standard for single-access 5-kHz and 25-kHz UHF satellite communications channels." Tech. Rep. MIL-STD-188-181B, Department of Defense, March 1999.

[11] Range Commanders Council Telemetry Group, Range Commanders Council, White Sands Missile Range, New Mexico, *IRIG Standard 106-00: Telemetry Standards*, 2000. (Available on-line at http://www.ntia.doc.gov/osmhome/106.pdf).

[12] T. Hill, "A non-proprietary, constant envelope, variant of shaped offset QPSK (SOQPSK) for improved spectral containment and detection efficiency," in *Proc. IEEE MILCOM*, Oct. 2000.

[13] M. Simon, *Bandwidth-Efficient Digital Modulation With Application to Deep-Space Communication*. New York: Wiley, 2003.

[14] *Appendix M, IRIG Standard 106-04: Telemetry Standards*, Range Commanders Council Telemetry Group, Range Commanders Council, White Sands Missile Range, New Mexico, 2004. (Available on-line at http://www.ntia.doc.gov/osmhome/106.pdf).

[15] L. Li and M. Simon, "Performance of coded OQPSK and MIL-STD SOQPSK with iterative decoding," *IEEE Trans. Commun.*, vol. 52, pp. 1890–1900, Nov. 2004.

[16] R. Schober and W. H. Gerstacker, "Metric for noncoherent sequence estimation," *Electron. Lett.*, vol. 35, pp. 2178–2179, Dec. 1999.

[17] L. Lampe, R. Schober, and M. Jain, "Noncoherent sequence detection receiver for Bluetooth systems," *IEEE J. Select. Areas Commun.*, vol. 23, pp. 1718–1727, Sept. 2005.

[18] E. Perrins and M. Rice, "Multi-symbol noncoherent detection of multi-h CPM," in *Proc. Int. Telemetering Conf.*, (Las Vegas, NV), Oct. 2003.

[19] D. Raphaeli and D. Divsalar, "Noncoherent detection of continuous phase modulation using overlapped observations," in *Proc. IEEE Global Telecommunications Conf.*, pp. 191–195, Nov. 1994.

[20] E. Perrins, T. Nelson, and M. Rice, "Coded FQPSK and SOQPSK with iterative detection," in *Proc. IEEE MILCOM*, (Atlantic City, NJ), Oct. 2005.